DIELECTRIC PERMITTIVITY MEASUREMENTS OF GEOLOGIC SAMPLES AT VENUS SURFACE TEMPERATURES. M. Barmatz[1], D. C. Nunes[1], J. Batres[1], M. Gilmore[2], D. Steinfeld[1], and J. Filiberto[3]. [1]Jet Propulsion Laboratory, California Institute of Technology, Pasadena CA, USA (martin.b.barmatz@jpl.nasa.gov); [2]Wesleyan University, Middletown, CT, USA; [3]Astromaterials Research and Exploration Science, NASA Johnson Space Center, Houston, TX, 77058, USA.

Introduction: Synthetic-aperture radar (SAR) and radar sounding are two powerful remote sensing techniques used to examine the surface and subsurface of planets. Their value is critical in the case of Venus due to this planet's global and visually opaque cloud layer. The recently selected VERITAS and EnVision orbital missions, slated to study the planet in the early 2030's, employ radar instruments to image the surface (VERITAS and EnVision) and probe the subsurface (EnVision). For both techniques, the complex dielectric permittivity of the surface and subsurface materials control radar backscatter intensity and penetration depth.

Since the 1970's, many studies have characterized the dielectric permittivity of geologic materials collected both on Earth and on the Moon to constrain the radar reflectivity and transparency at a variety of radar frequencies [e.g., 1]. Two consistent findings from those studies are that complex permittivity depends on both the density (or porosity) and the composition of the material. Denser materials and more metal-rich compositions tend to have higher permittivity values and to incur greater propagation path loss. Water content also elevates permittivity of otherwise dry rocks/soils/regolith [e.g., 2]. However, permittivity is independent of frequency for the 0.5-18 GHz range [3], within which SAR imaging commonly lies.

The one aspect poorly explored thus far is the effect of elevated temperatures on dielectric permittivity. Previous work [4, 5, 6] suggests that increased lattice vibrations and flow of free electrons associated with an increase in temperature elevate both the real (reflectivity) and imaginary (path loss) parts of the complex permittivity.

We are currently conducting a 3-year campaign to measure the complex dielectric permittivity of Venus-relevant geologic materials at Venus surface temperatures (380°C - 460°C) and with frequencies relevant to VERITAS, EnVision, and Magellan imaging synthetic aperture radars.

Samples: Several Soviet Venera and Vega landers performed chemical analyses of the surface materials that are consistent with basalt and alkali basalt, with varying amounts of alteration through chemical weathering with the lower atmosphere [7]. The basaltic interpretation is corroborated by the morphology of lava flows found to cover most of the surface, as imaged by Magellan [8]. A much smaller, but non-negligible portion of the surface of Venus is dominated by heavily tectonized tessera terrain, which NIR emissivity data from Venus Express suggests having a more felsic composition, perhaps granitic, than the mafic volcanic rocks found in the plains [9].

To capture the possible range of rocks and minerals thought to exist on the surface of Venus, our experiments include mafic and felsic igneous rocks, their constituent minerals and some minerals predicted to occur due to surface weathering. Because permittivity depends on density, we measure the samples at a range of grain sizes/packing and, cores.

Experimental Approach: We employ the resonant cavity perturbation method (ASTM D2520) to measure the complex permittivity of the material outlined. The rectangular resonant cavity is tuned to resonate in several transverse-electric TE_{10n} modes near 2.45 GHz. This custom-made brass cavity is placed inside a Sentro Tech oven capable of sustaining temperatures between 23°C and 460°C (Fig. 1) needed for this study.

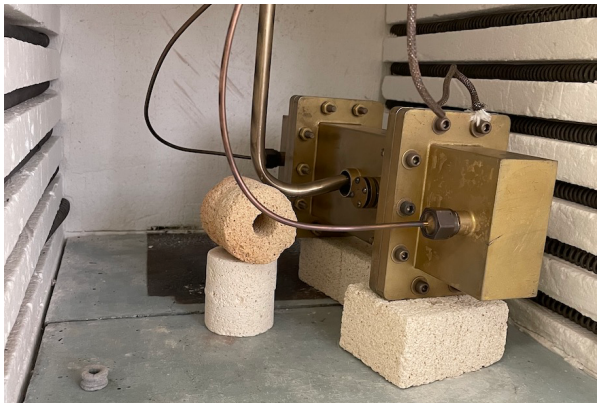

Fig. 1 *– Resonance cavity (golden box with bolted flanges) within oven, ready for a high temperature run.*

The cavity is connected to a Keysight Vector Network Analyzer (VNA) to obtain the four S-parameters, from which the quality factor Q of the resonance is obtained. The approach entails measuring Q at each desired temperature first with the cavity empty of sample, and then with the cavity loaded with the sample (Fig. 2). Insertion of a sample in the cavity reduces Q and the frequency f at which the resonance occurs. The real and imaginary parts of the complex permittivity are then calculated from the frequency and magnitude of Q for both empty and sample-loaded conditions, or:

Real part: $\varepsilon' = V_c \frac{f_c - f_s}{2V_s f_s} + 1$

Imaginary part: $\varepsilon'' = \left(\frac{V_c}{4V_s}\right)\left(\frac{1}{Q_s} - \frac{1}{Q_c}\right)$.

Subscripts c and s correspond to empty cavity and sample, respectively, while V, Q, and f denote volume, Q-factor peak value, and resonance frequency.

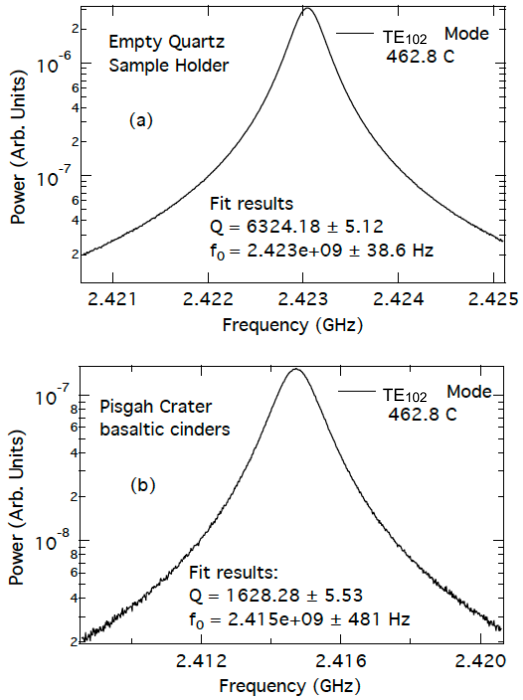

***Fig. 2** – Resonance Q factor and frequency for a basaltic sand sample at ~460°C for both empty (top) and loaded sample (bottom) conditions. The basaltic sample had a density of 1.17 g/cm³.*

The uncertainty in the setup is expressed in the values of Q and f, and they lie in the order of < 0.5%.

Overall, the resonant cavity method is rather fast, precise, and simple to execute. It is the thermal cycling that imposes the greatest demand on the experiment. To achieve and stabilize the cavity at a given desired temperature from 23°C to 460°C, and then cool it back down to room temperature, each run takes approximately 2 days to execute.

Results: At the time of this writing, we have measured 10 different rocks and minerals, spanning the mafic and felsic compositional ranges (olivine, bytownite, apatite, basalt, granite), as well as some potential weathering products (hematite and pyrite). As previously established throughout the literature, density increases permittivity, as shown in Fig. 3, but our real-part permittivity values tend to be higher than the usual 1.92^{ρ} rule and values reported in [1].

The real part of the permittivity also increases with increasing temperature. This is most noticeable at the higher densities, where the real part of the permittivity increases 5% at a density of 1.17 g/cm³, and 15% at a density of 2.62 g/cm³. Because temperature has no effect on free-space, at lower densities where the free-space volume fraction is substantial, the temperature-induced variation is smaller. Further, the spread induced by temperature is comparable, if not larger, than the scatter found in [1] at similar densities, so the thermal effect is non-negligible and needs to be accounted for when interpreting radar data.

Qualitatively, the trends are similar for the imaginary parts of permittivity, higher with the increase of both density and temperature. However, the quantitative trends are not as clear as for the real parts. For example, for the Saddleback core case, the imaginary part is nearly constant with temperature.

Plan Forward: Results shown herein show a mix of different samples at different densities, obtained during the first year of effort. In this second year, we are currently working to measure the same samples at different densities, so we can exclude compositional effects when obtaining trends. We will also continue to measure a wider sample set that will encompass analogues for the plains, tessera, and weathered surface of Venus.

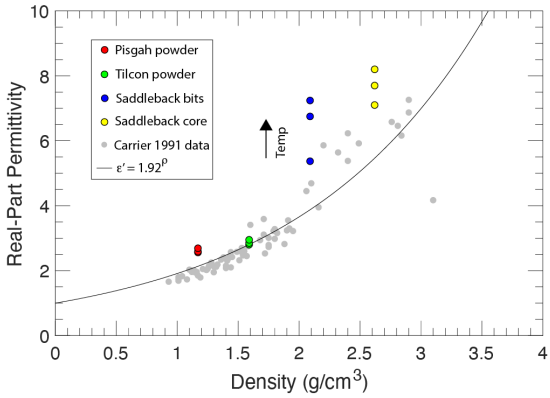

***Fig. 3** – Real-part permittivity results (colored) from our experiments on basalts at different densities and temperatures. Power-trend (line) and gray dots correspond to those in [1] for different samples measured from 450 MHz to 9 GHz. Measurements were taken at 23°C, 230°C, and 460°C.*

Acknowledgements: This work is supported by a NASA PDART grant to JPL. Samples come from collections at Wesleyan (Gilmore) and JPL (Nunes). We also thank Darby Dyar for mineral samples, sorted to multiple grain sizes.

References: **[1]** Carrier W. D. et al. (1991), in *Lunar Sourcebook*, Cambridge U. Press. **[2]** Olhoeft G. R. et al. (1975), *LPSC 6*, p. 3333-3342. **[3]** Ulaby F. T. et al. (1990), *IEEE-TGRS 28*, p. 325-336. **[4]** Havinga E. E. (1961), *J. Phys. Chem. of Solids 18*, p. 253-255. **[5]** Cygan R. T. and Lasaga A. C. (1986), *Am. Mineralogist 71*, p. 758-766. **[6]** Yushkova O. V. and Kibardina I. N. (2017), *Solar Sys. Res. 51*, p. 121-126. **[7]** Fegley B. (2003) in Treatise on Geochemistry, 487. **[8]** Ford J. P. and Plaut J. J. (1993), *JPL Publication 93-24*. **[9]** Gilmore M. S. et al. (2015) *Icarus 254*, 350.